Archives of Dermatological Research (2023) 315:751–760
https://doi.org/10.1007/s00403-022-02408-1

ORIGINAL PAPER

Reverse-traction skin-stretching device for primary closure of large skin defects

Yutao Cui[1] · Baoming Yuan[1] · Yan Zhang[1] · Guangkai Ren[1] · Minghan Dou[1] · Chuangang Peng[1] · Dankai Wu[1]

Received: 2 April 2022 / Revised: 23 August 2022 / Accepted: 13 October 2022 / Published online: 21 October 2022

Abstract

The tension in the skin margin of a wound is the major determinant for wound healing. The difficulty of primary closure for large skin defects due to excessive wound tension has long been a clinical challenge. In this study, we designed and fabricated a reverse-traction skin-stretching device (RT-SSD) to relieve the skin tension of a large skin defect and thereby allow primary wound closure. The novel RT-SSD designed in this study drives the fixing device fixed on the skin edge of the wound by rotating the pulling device, thus exerting a reverse tensile force on both sides of the wound, causing creep and stress relaxation, thus reducing the skin tension. Through the tension analyses; microcirculation detection; clinical scores; and a series of histological staining in vivo, it is verified that intraoperative application of RT-SSD can stretch and straighten collagen and fragment elastin, thus effectively reducing skin tension of large skin defect of miniature pigs. In addition, its special linear and planar traction protects the subcutaneous microcirculation of the wound site. The evaluation of wound healing confirmed that RT-SSD had negligible negative impact on wounds, reduced the incidence of complications, and promoted the healing of large skin defects. Therefore, this study provides a new safe and effective device for the primary closure of large skin defects.

Keywords Skin-stretching device · Large skin defect · Skin tension · Wound closure

Introduction

Large skin defects caused by severe trauma and burns lead to patients experiencing significant pain and present considerable challenges in the clinical treatment given their difficulty in primary closure and increased risk of infection [1–3]. To address this issue, a variety of treatment methods including flap reconstruction, skin graft, tissue expansion, and other methods were used to achieve wound closure through secondary surgeries [4–7]. However, traditional treatment methods of secondary surgeries are intricate, the risks of these treatments are high, and additional skin donor areas are required. In addition, in the healing area, numerous scars often remain, the healing tissue is not wear resistant, and the sensory function is often difficult to recover [8, 9]. Therefore, the application of a skin stretch technique provides a relatively simple and appropriate method for primary closure of large defects.

The skin stretch technique is a treatment strategy based on the inherent biomechanical characteristics of the skin, wherein the healthy skin is extended to the opposite side of the defect, and the wound is closed by applying a controlled and evenly distributed pull along the edge of the healthy skin [10, 11]. The skin has biomechanical properties of extensibility and viscoelasticity, which cause it to stretch when applied with a traction load and to recoil when the load is removed. Moreover, skin also has the characteristics of mechanical creep and stress relaxation. When the skin is stretched up to a certain distance and maintained for a sufficient duration, the tension that keeps the skin stretched and recoiled decreases slowly over time, resulting in permanent skin extension [12, 13]. In the recent decades, a variety of skin stretch devices (SSD) have been designed and successfully used in the clinic. These SSDs can be used continuously or intermittently during or after surgery [14]. SSDs effectively eliminate the problems of skin donor surgery and complications. However, the commonly used clinical SSDs mostly span the wound and are inserted into the skin margin

✉ Dankai Wu
wudk@jlu.edu.cn

[1] Orthopaedic Medical Center, The Second Hospital of Jilin University, Changchun 130041, People's Republic of China

where they pull the edge of the wound by point traction. This kind of traction can cause great damage to the skin margin, leading to an increased incidence of skin necrosis, dehiscence, and delayed healing [10]. Furthermore, the pulling force of this point traction is limited, which causes the skin to be pulled for a long time, damaging the local blood supply.

In the present study, a reverse-traction SSD (RT-SSD) was designed and developed for primary closure of large skin defects by linear traction or planar traction. By rotating a handle, this RT-SSD can be made to pull the fixing device on both sides of the wound, thereby applying a double reverse pulling force to close the wound. The fixing device on the wound margin enables the skin traction force to be uniformly distributed; thus, linear or even planar pulling can be performed, resulting in enhanced pulling force and reduced damage to the edge of the wound. The effect of traction and healing promotion of RT-SSD on large skin defects were evaluated by mechanical analysis, clinical standard, and histological analysis in vivo. We hypothesized that RT-SSD may effectively reduce the tension of a large skin defect and reduce the necrosis of the skin margin, thereby achieving primary closure of the large skin defect and preventing local complications in the wounds site.

Materials and methods

Materials

Stainless-steel wires used for the fabrication of RT-SSD were purchased from Yuansheng Stainless Steel Products Co. Ltd (Jiangsu, China). The carbon fiber used to make the RT-SSD traction device was provided by Yucai Technology Co. Ltd (Changchun, China). The sutures used to secure the wound were purchased from Johnson & Johnson Co. Ltd (New Jersey, USA). Paraformaldehyde for skin tissue fixation was purchased from Solarbio Technology Co. Ltd (Beijing, China).

Design and fabrication of RT-SSDs

The RT-SSD designed in this study consists of a reverse traction device, a connecting device and a fixing device. The working process of RT-SSD is mainly to first fix the fixing device symmetrically to the edges of both sides of the skin defect. The fixing device consists of a stainless-steel wire to connect with the traction device via the connecting device and a stress buffering device consisting of a silicone tube sleeved outside the stainless-steel wire. The connecting device is mainly composed of two fixing holes integrated with the traction device and two fixing screws. The stainless-steel wires provide the RT-SSD with the necessary strength during the traction process. The two end parts of the stainless-steel wires located on both sides of the skin defect respectively penetrate into the fixing holes and are fixed by the screws. The stress-buffering silicone tubes are sleeved outside the stainless-steel wire and symmetrically fixed to both sides of the skin margin by suturing using surgical suture; thus completing the installation of RT-SSD on the wound. The reverse traction device consists of a rotatable sleeve handle and a movable device that is fixed inside the handle by threads. By rotating the handle, the two parts move away from each other and the reverse traction device is extended. Subsequently, the fixing devices in both sides can be tightened by the extended reverse traction device to approach each other, so that the skin at both sides of the wound can be indirectly stretched. Furthermore, by changing the number of fixation devices on the same side of the wound, RT-SSD can perform linear traction or planar traction, to change its traction force and have an impact on the local skin. The demonstration of RT-SSD is shown in Fig. 1. The reverse traction devices for RT-SSD were manufactured and provided by Yucai Technology Co. Ltd (Changchun, China).

Surgical procedures

All animal assessments were conducted in compliance with Chinese laws and regulations on animal experiments, and all experimental protocols were approved and performed according to the guidelines of the Animal Ethics Committee of Jilin University. Nine healthy, 10-month-old miniature pigs with no significant difference in weight were used for the in vivo study. The pigs were housed in cages and had ad libitum access to food and water. A large oval skin defect measuring 6×8 cm was created at the same location on the dorsal region of each pig by removing the entire skin and subcutaneous tissues using a dermatome. This size of the skin defect was proven incapable of direct suturing during the operation by the pinch test. We used a push – pull testing device (Handpi instrument Co., Ltd, Zhejiang, China) to detect the tension around each wound to ensure the consistency of each wound before treatment. After making skin defects, all experimental animals were randomly divided into three treatment groups: control group, group receiving reverse-traction SSD with single fixing device (RT-SSD/SF), and group receiving reverse-traction SSD with double fixing device (RT-SSD/DF). In the control group, after full-thickness skin resection, a high-tension suture was directly performed with surgical suture. In the RT-SSD/SF group, a fixing device was installed on each side of the wound to perform a linear traction on the wound. In the RT-SSD/DF group, two fixation devices were installed on each side of the wound to allow for planar traction of the wound. After the SSD was installed in RT-SSD/SF and RT-SSD/DF groups,

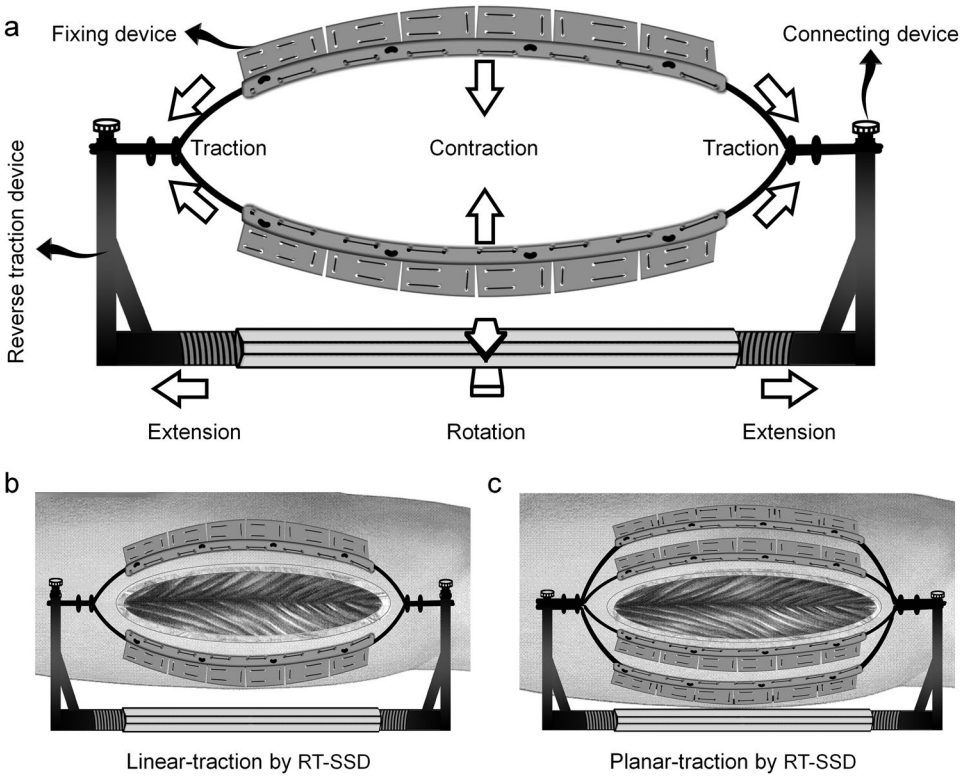

Fig. 1 Illustration of the working process of reverse-traction skin stretch devices (RT-SSD): **a** By rotating the shaft of the reverse traction device, it can be lengthened, thus exerting a reverse traction force on the fixation device, resulting in skin tractions around the wound. RT-SSD can perform linear traction (**b**) or planar traction (**c**) by changing the fixing device in the two sides of the skin defect

the tractions were cyclically performed. Specifically, the traction device was rotated to stretch the skin edges of the wound tending to be completely aligned and maintained for 4 min. Then, to further reduce the impact on the blood supply to the skin edges, the traction device was restored to its original position and maintained for 60 s. The traction of the wound was continued in the cycle of 4 min traction with 60 s intermission. After preliminary confirmation by pinch test that a significant reduction in wound tension was sufficient for closure, the tractions were stopped and the wound tensions were remeasured. The wounds were sutured after the SSDs were removed. After suturing in each group, the wounds were covered with sterile gauze, and the dressings were changed regularly. To prevent infection, penicillin was given by intramuscular injection (50,000 IU/kg) within 3 days after surgery.

Evaluation of microcirculation around wound

To study the effect of treatment in each group on the microcirculation of wound margin, the percutaneous partial pressure of oxygen ($TcpO_2$) at the wound margin was measured. Before large dorsal skin defects were created, TcpO2 was tested to determine the control baseline for normal skin microcirculation in each group. After the wounds were treated and sutured in each group, the changes of TcpO2 of skin wound edges were detected and compared.

Analysis of microstructural changes around wound

According to the stitches removing time in back site required clinically, the defect site and surrounding skin were harvested to evaluate the stretch effect and wound healing after 10 days of surgery. The skin samples were harvested and fixed in 4% paraformaldehyde solution. Then, the fixed samples were dehydrated in a graded ethanol series and embedded in paraffin according to routine histological processing. Sample blocks were sectioned at a thickness of 5 μm for Masson's trichrome and Verhoeff – Van Gieson (VVG) staining to further study the collagen bundles and elastin in the dermis of the skin surrounding the defect site after traction.

Clinical scores for wound healing

A modified clinical skin healing score was used to evaluate the healing of each group on the 10th day after the operation. The scoring criteria were as follows: No obvious reaction, 1 point; slight swelling or erythema, 2 points; suture inflammation of at least 1-cm thickness, 3 points; abscess formation, 4 points; and incision dehiscence, skin necrosis, or wound closure, 5 points [15]. Scores were recorded and counted by physicians who were blinded to the experimental groups.

Histological analysis of wound healing

To further confirm the tissue regeneration of the defect, the complete skin and subcutaneous tissue of the defect site were taken out and fixed in 4% paraformaldehyde solution on the 10th day after the operation. Subsequently, the fixed tissue was dehydrated in a gradient ethanol series, embedded in paraffin, and then cut into 5-μm-thick tissue sections. Then, hematoxylin – eosin staining (HE) and Masson's trichrome staining was used to evaluate the morphology and condition of the healing tissue in the defect site.

Statistical analysis

All data are represented as the mean ± standard deviation (SD) from three independent experiments. Statistical analysis was performed using the independent samples *t* test by SPSS 19.0 software (IBM, Armonk, NY, USA). $P < 0.05$ was considered to indicate a significant difference among groups**.**

Results

Traction effect of RT-SSD on the wound

Effect of RT-SSD on wound tension

In this study, a 6 × 8 cm large oval skin defect was successfully created on the dorsal region of the miniature pig. We confirmed that the skin tension in the dorsal region of animal was maximum, and the wound was confirmed to be unsuited for direct closure based on the pinch experiment (Fig. 2). In the control group, direct wound suture was then performed. However, the wound tension was very high and the primary closure was not complete. Ultimately, the incision had a residual gap with a maximum distance of 1.3 ± 0.2 cm that could not be completely aligned. In the RT-SSD/SF group, after the SSD was installed, the pull was performed cyclically for 4 min with 60 s intervals, and the wound was completely closed after eight continuous cycles. In the RT-SSD/DF group, after the SSD was installed, the pull was performed cyclically for 4 min with 60 s intervals, and the wound was completely closed after four cycles (Fig. 2). We studied the changes in skin tension before and after treatment with RT-SSD using a push – pull testing device. Before treatment, the wound tension in each group was basically the same, which was 26.6 ± 1.1 N in the control group, 25.7 ± 2.8 N in the RT-SSD/SF group, and 26.9 ± 1.8 N in the RT-SSD/DF group. After treatment, the wound tensions in the RT-SSD/SF and RT-SSD/DF groups were 8.8 ± 0.5 N and 7.4 ± 0.6 N, respectively, which were significantly lower than those in the control group before primary wound closure; the wound tension in the RT-SSD/DF group was the lowest (Fig. 3).

Effect of RT-SSD on microcirculation

$TcpO_2$ was measured to evaluate the effect of the application of RT-SSD on the microcirculation of the skin margin. As shown in Fig. 4, the normal $TcpO_2$ in the dorsal region of miniature pig was 50.94 ± 1.44, 52.63 ± 2.03 and 54.00 ± 2.21 mmHg respectively. After different treatments, $TcpO_2$ decreased to 12.02 ± 5.75, 34.64 ± 4.04 and 44.73 ± 2.09 mmHg in the CON, RT-SSD/SF and RT-SSD/DF groups respectively. The direct suture method in CON group significantly decreased the blood supply of the skin margin, which was lower than that in the two RT-SSD treatment groups. The degree of $TcpO_2$ reduction in the RT-SSD/DF group was significantly lower than that in the RT-SSD/SF group. This indicated that the traction of RT-SSD had an acceptable effect on the blood supply and that the RT-SSD/DF group had the lowest effect on the blood supply in traction area.

Microstructural changes in the dermis

After 10 days of surgery, the miniature pigs in each group did not show any obvious complications such as abnormal activity, behavior and weight changes. Therefore, all the experimental animals were included in the follow-up studies. We further studied the effect of RT-SSD on skin traction by observing collagen fibers with Masson's trichrome staining and elastin with VVG staining in the dermis of the skin around the wound. As shown in Fig. 5a, collagen fibers in the RT-SSD/SF and RT-SSD/DF groups were more parallel to each other than those in the control group, and more undulated collagen was straightened, while elastin showed more fragmentation. Subsequent semi-quantitative analysis also supported the above results. The average length of the collagen fibers in the RT-SSD/SF and RT-SSD/DF groups was significantly higher than that in the control group, and was highest in the RT-SSD/DF group. Whereas, the average length of elastin in the RT-SSD/SF and RT-SSD/DF groups was significantly lower than that in the control group (Fig. 5b, c).

Evaluation of wound healing

Clinical score of wound healing

To study the healing of large skin defects after treatment in each group, clinical scoring and histological analysis of wound healing were carried out. Clinical scoring was performed on the 10th postoperative day based on the superficial appearance of the wound site. In the control group, the

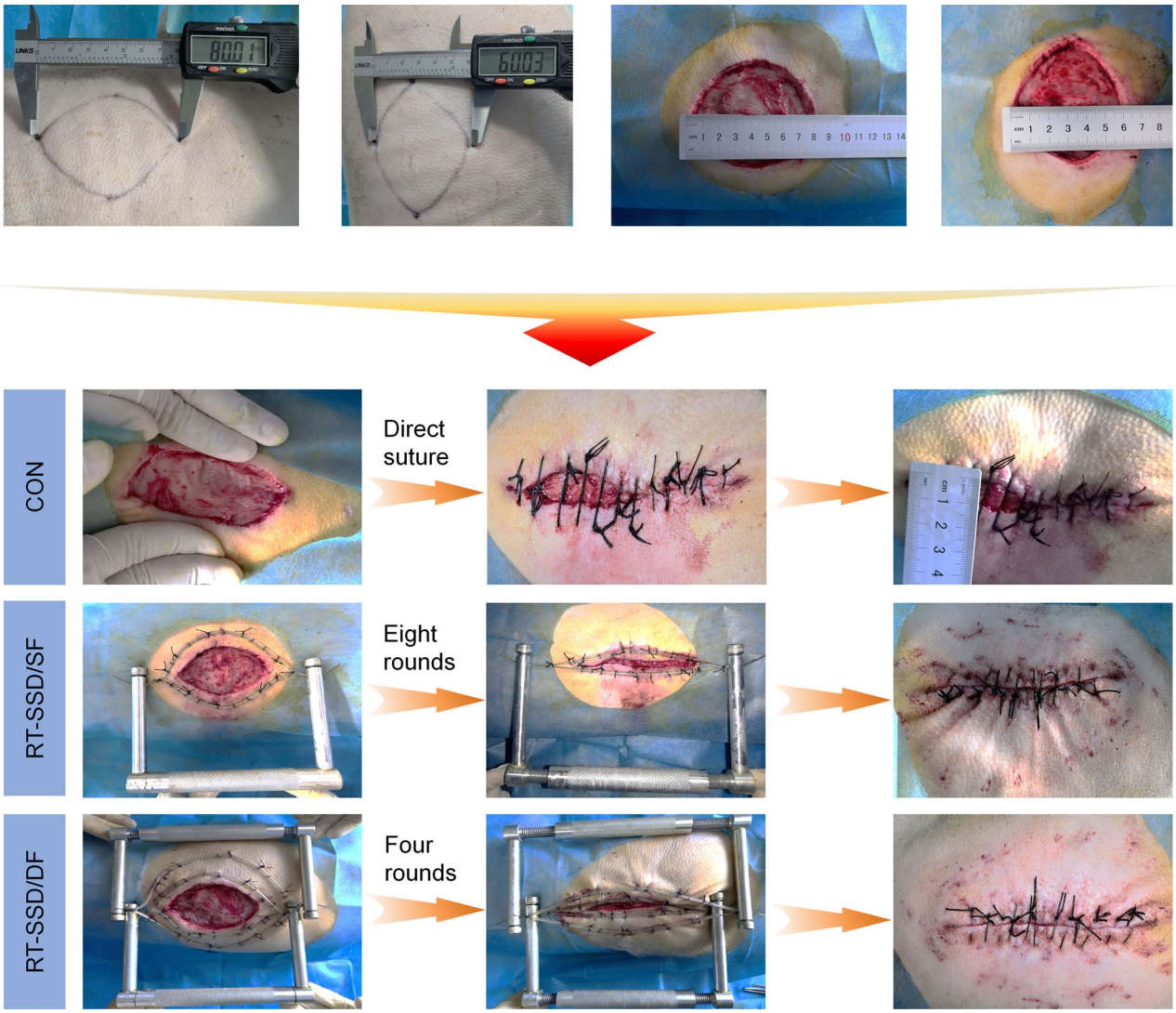

Fig. 2 Description of the primary closure process for large skin defects in the control (CON), linear traction (RT-SSD/SF), and planar traction (RT-SSD/DF) groups

wound could not be completely closed due to the excessive tension. Therefore, after removing stitches on postoperative day 10, the wound failed to form a stable fibrous tissue connection, resulting in wound dehiscence; some wounds showed abscesses and necrosis. However, in the RT-SSD/SF and RT-SSD/DF groups, the skin almost healed without dehiscence, and no obvious complication such as abscess was observed after the stitches were removed on postoperative day 10 (Fig. 6a). Thus, the clinical scores in the RT-SSD/SF and RT-SSD/DF groups were 1.7 ± 0.6 and 1.3 ± 0.6, respectively, which were significantly lower than 4 ± 1 in the control group. However, the clinical scores between the RT-SSD/SF and RT-SSD/DF groups showed no significant statistical difference (Fig. 6b). This showed that from the dimension of superficial appearance, the treatment with the RT-SSD promoted wound healing, but no difference in appearance of wound healing between the linear and planar traction groups was observed.

Histological analysis

Histological analyses performed after HE and Masson's trichrome staining at postoperative 10 days are shown in Fig. 7. In the control group, histological analysis showed that the skin epidermis was damaged, several acute and chronic inflammatory cells infiltrated the dermis, and the collagen fibers were significantly broken. In the RT-SSD/SF group, the spinous layers of the skin epidermis were hyperplastic to repair the wound, and dermal fibrous histiocytes proliferated with focal inflammatory cell infiltration. In the RT-SSD/DF group, the epidermis of the wound healed, and thick collagen fibers proliferated in

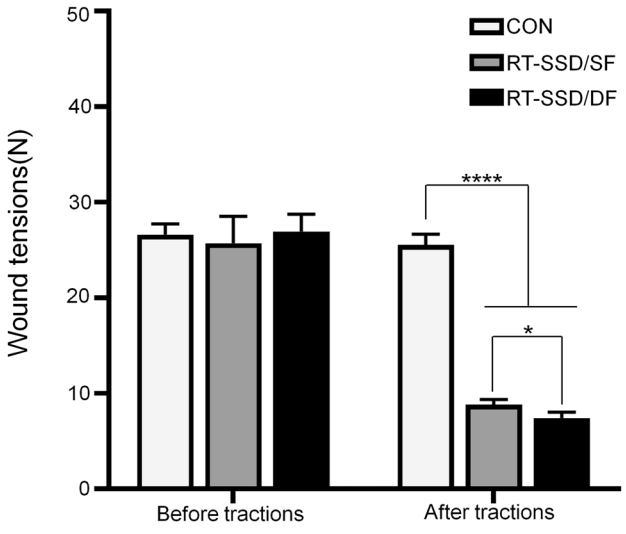

Fig. 3 The changes in wound tension of large skin defects before and after treatment with RT-SSD ($n=3$, *indicates significant differences between the groups, $^{*}P<0.05$, $^{****}P<0.0001$)

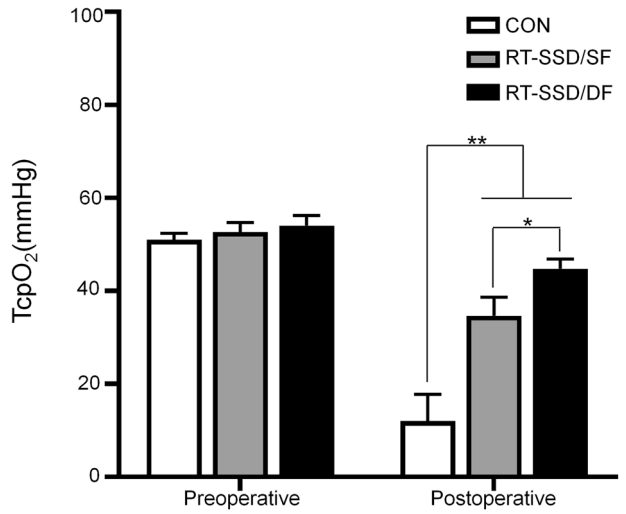

Fig. 4 The changes of TcpO2 of the skin margin around the wound before and after operation ($n=3$, *indicates significant differences between the groups, $^{*}P<0.05$, $^{**}P<0.01$)

the dermis, with a large amount of scar formation and a small amount of inflammatory cell infiltration. Therefore, histological analysis confirmed that wound healing in the control group was the worst, and skin damage was still evident, despite formation of granulation tissue. The two groups treated with RT-SSD had better healing than the control group, with the RT-SSD/DF group having the best healing and almost complete healing on day 10.

Discussion

The treatment of large skin defects has always been a complex medical problem. In these cases, skin tension at the edge of the wound is a determining factor for wound healing. The tension of wound closure in large defects is high, which makes the primary wound closure difficult, resulting in increased incidence of skin necrosis, wound nonunion, infection, and other complications [16–18]. In this study, we designed a safe and effective RT-SSD using a simplified operation. We evaluated the function of RT-SSD for wound healing in miniature pigs with large skin defect. Owing to stress relaxation, wound tension was reduced 65.8% after 8 traction cycles (traction for 32 min) with RT-SSD/SF and 72.5% after 4 traction cycles (traction for 16 min) with RT-SSD/DF. This result has a similar stress relaxation effect to a previous study with a clinical commercial SSD, which achieved a 65% reduction in tension after stretching the human scalp for 30 min [19]. Therefore, RT-SSD can effectively reduce the wound tension of large skin defects, and RT-SSD/DF has increased traction efficiency. This is because the RT-SSD/DF group had more tissues around the wound under traction than the RT-SSD/SF group, when the traction device of RT-SSD was extended by the same distance.

During the use of the SSD, skin necrosis can be caused given the fact that continuous traction force can compress the skin margin and interrupt blood supply [20–22]. The linear and planar traction of RT-SSD can reduce the pressure on the skin's edge via more even stress distribution. In addition, the intraoperative recycling application can greatly improve the situation, thus preventing necrosis of the skin margin. By symmetrically adding fixing devices, the RT-SSD can make the stress distribution more uniform, so its influence on $TcpO_2$ is least. RT-SSD has negligible effect on the blood supply of skin margin.

The mechanism of RT-SSD reducing wound tension was studied by elevating the microstructural changes in the dermis. The dermis is mainly composed of tightly packed collagen fibers, elastin fibers, and trace amounts of reticulin and ground substance, which endows the skin with certain firmness, tensile strength, and recoil ability [23–26]. Collagen fiber and elastic fiber are two important protein fibers in dermis, and they have different properties and functions [12]. Collagen fibers have high tensile strength and lack extensibility; therefore, they mainly contribute to the structural support of the skin. In the relaxed state, the collagen fibers are arranged in a disorderly pattern within the ground substance. When the skin is stretched, the collagen fibers are aligned parallel to each other, and under tensile strain, the undulated collagen fibers are straightened [12, 27]. Elastin fibers have strong elasticity and

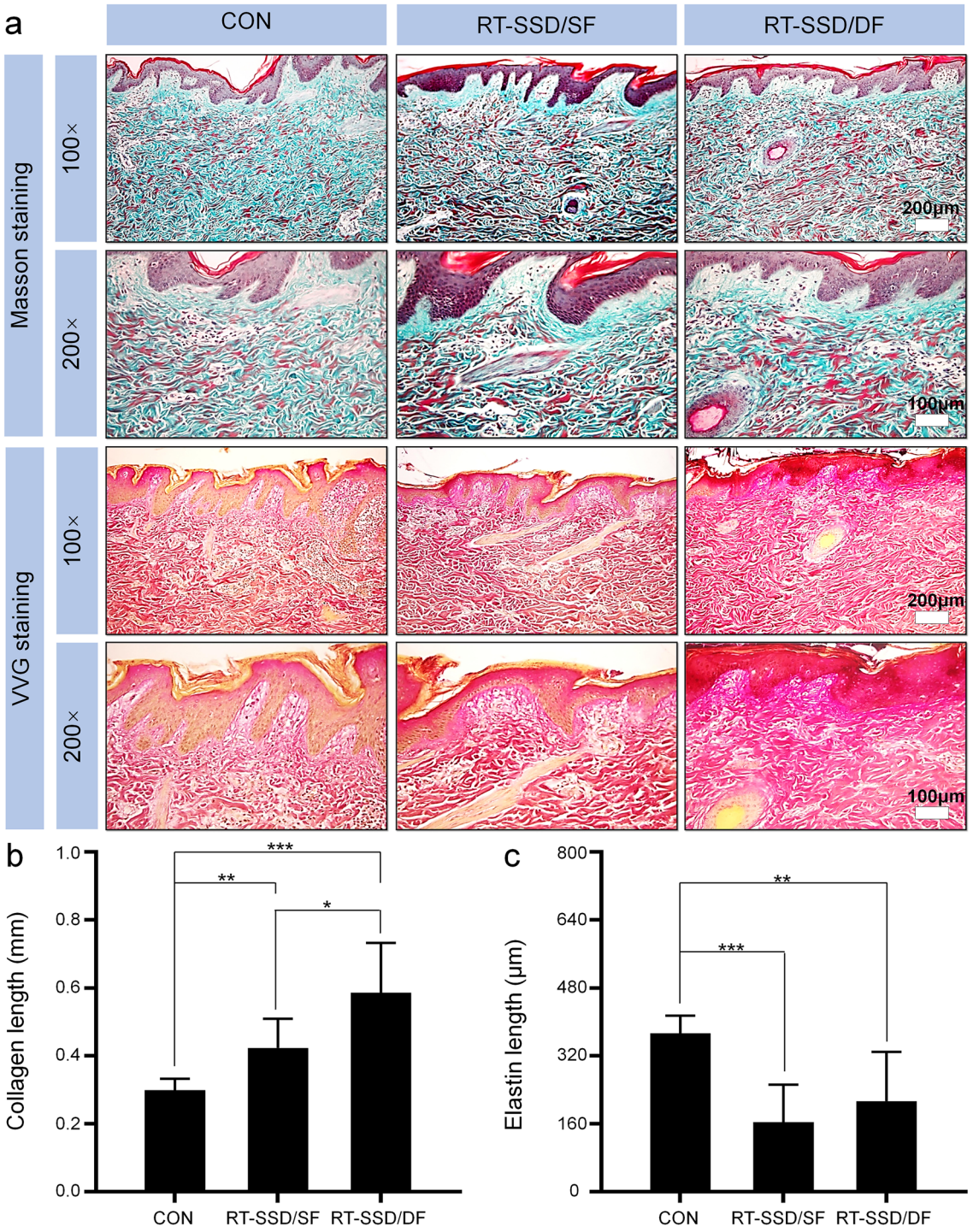

Fig. 5 Analysis of skin stretching effect of RT-SSD: **a** Masson staining for collagen and VVG staining for elastin in the dermis of CON, RT-SSD/SF, and RT-SSD/DF groups; Semi-quantitative analysis of the lengths of collagen (**b**) and elastin (**c**) in the dermis of CON, RT-SSD/SF, and RT-SSD/DF groups, with ImageJ analysis. ($n=3$, *indicates significant differences between the groups, $^{*}P<0.05$; $^{**}P<0.01$, $^{***}P<0.001$)

extensibility, along with the ability to restore its original shape after strain, which gives the skin its ability to recoil. Moreover, elastin fibers can also contact with collagen fibers to promote collagen fibers to restore its undulated shape after the strain is removed. However, when sufficient and effective stretch is performed, the elastin fibers can be fragmented, resulting in a loss of the skin's recoiling properties [20, 28]. The use of RT-SSD resulted

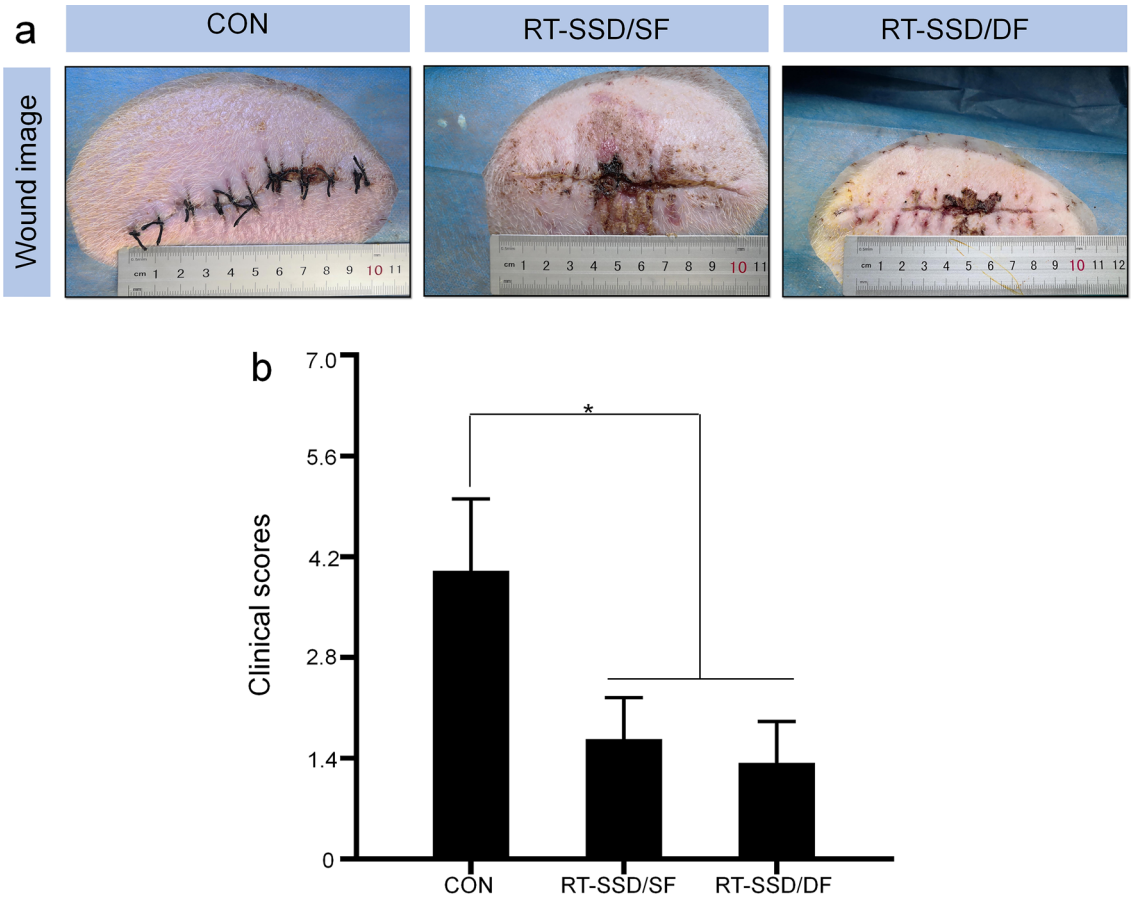

Fig. 6 Evaluation of wound healing: Representative image (**a**) and clinical scores (**b**) for wound healing in the CON, RT-SSD/SF, and RT-SSD/DF groups on postoperative day 10 ($n=3$, *indicates significant differences between the groups, $*P<0.05$)

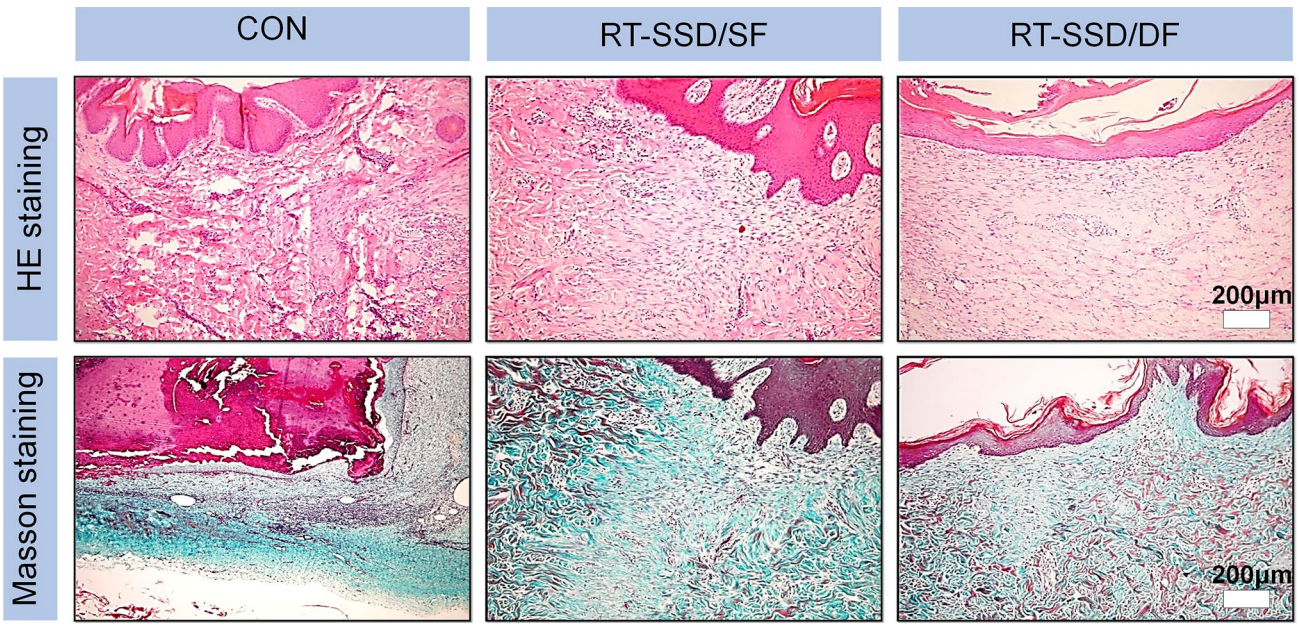

Fig. 7 HE and Masson staining of the wound sites on postoperative day 10 in the CON, RT-SSD/SF, and RT-SSD/DF groups ($n=3$)

in straightened and elongated collagen and fragmented elastin. These changes cause stress relaxation of the skin, thereby significantly reducing the wound tension.

An appropriate local microenvironment is essential for the healing of skin defects. Direct suture is an effective method to close skin defects and promote wound healing, especially when there is no tension in the wound [9, 29]. However, in large skin defects, excessive tension makes direct suture difficult to achieve. In this study, the forced direct suture resulted in necrosis of the skin margin, a large infiltration of inflammatory cells, and inhibited wound healing. The application of RT-SSD enabled the wound to achieve primary closure in a low-tension microenvironment. Primary wound closure greatly reduces the risk of complications such as infection which can also be a major impediment to wound healing [30]. Furthermore, the low-tension microenvironment reduces the blockage of blood supply to the defect site, thereby avoiding necrosis and promoting wound healing.

However, this study also has certain limitations. Due to the greater fragility of human skin relative to miniature pigs, tearing of the skin is more likely to occur when stretching skin defects of the same size. Therefore, in future study, we will quantify the magnitude of the traction force to determine the safety threshold for clinical use of RT-SSD. Moreover, we prepared a regular wound via full-thickness skin resection, while in clinical practice, the skin trauma would be more complex, such as the occurrence of skin degloving injury or other cases of poor blood supply at the skin margin. In these cases, RT-SSD might be more likely to affect the blood supply of the skin margin, so we will further study the effects of RT-SSD in these complex environments.

Conclusion

In this study, we designed and manufactured a skin stretch device that released wound tension by reverse traction for successful primary closure of a large skin defect. The RT-SSD was confirmed to have an appropriate skin-stretching effect, effectively reducing the wound tension of large skin defects, allowing primary wound closure; moreover, it protected subcutaneous microcirculation, had negligible negative effects, reduced the occurrence of complications, and resulted in enhanced skin healing. The linear traction and planar traction could be performed by changing the number of fixing devices to adjust the traction force and the pressure on the local microcirculation of the RT-SSD. The planar traction had more superior traction effect and more dispersed stress on the wound, so it was suitable for the rapid closure of larger defects during surgery. We believe that RT-SSD has provided a new strategy for the healing of large skin defects and shows promising application prospects.

Author contributions YC: Conceptualization, Methodology, Investigation, Formal analysis, Writing-original draft, Data curation. BY: Writing-review and editing, Methodology. YZ: Resources, Methodology, Data curation. GR: Data curation, Investigation. MD: Writing—review and editing. CP: Funding acquisition, Writing—review and editing. DW: Conceptualization, Funding acquisition, Writing—review and editing, Supervision.

Funding This study was supported by Scientific Development Program of Jilin Province [20200404190YY, 20200404140YY] and Program of Jilin Provincial Health Department [2019SCZT014].

Declarations

Conflict of interest The authors declare that they have no conflict of interest.

References

1. Hung MH, Liao CT, Kang CJ, Huang SF (2017) Local rhomboid flap reconstruction for skin defects after excising large parotid gland tumors. J Oral Maxillofac Surg. 75(1):225 (**e1–e5**)
2. Li Z, Knetsch M (2018) Antibacterial strategies for wound dressing: preventing infection and stimulating healing. Curr Pharm Des 24(8):936–951
3. Ji X, Li R, Jia WY, Liu GM, Luo YG, Cheng ZQ (2020) Coaxial fibers with janus-structured sheaths by electrospinning release corn peptides for wound healing. ACS Appl Bio Mater 3(9):6430–6438
4. Kim SW, Choi SH, Kim JT, Kim YH (2015) An additional option for split-thickness skin graft donors: the previous free flap sites. Ann Plast Surg 75(6):634–636
5. Yan S, Shi H, Chen D, Guo J, Sun Y, Wu S (2018) Repair of large full-thickness scalp defects using biomaterial and skin grafting. J Craniofac Surg 29(4):e426–e429
6. Lorenzen MM, Gunnarsson GL, Bille C, Tos T, Koudahl V, Rindom MB et al (2019) Visualized bilateral breast reconstruction by propeller thoracodorsal artery perforator flaps. Gland Surg 8:S262–S270
7. Silva AK, Humphries LS, Maldonado AA, Gottlieb LJ (2019) Chimeric vs composite flaps for mandible reconstruction. Head Neck 41(6):1597–1604
8. Lee TJ, Oh TS, Kim EK, Suh H, Ahn SH, Son BH et al (2016) Risk factors of mastectomy skin flap necrosis in immediate breast reconstruction using low abdominal flaps. J Plast Surg Hand Surg 50(5):302–306
9. Song M, Zhang Z, Liu T, Liu S, Li G, Liu Z et al (2017) EASApprox(®) skin-stretching system: a secure and effective method to achieve wound closure. Exp Ther Med 14(1):531–538
10. Lei Y, Liu L, Du SH, Zong ZW, Zhang LY, Guo QS (2018) The use of a skin-stretching device combined with vacuum sealing drainage for closure of a large skin defect: a case report. J Med Case Rep 12(1):264
11. Lapid O (2006) An improvised wound closure system. J Trauma 60(4):910–914
12. Joodaki H, Panzer MB (2018) Skin mechanical properties and modeling: a review. Proc Inst Mech Eng H 232(4):323–343
13. Ali AK, Abubakar AA, Kaka U, Radzi Z, Khairuddin NH, Yusoff MSM et al (2018) Histological changes of immediate skin expansion of the distal limb of rats. Vet World 11(12):1706–1711
14. Verhaegen PD, van Trier AJ, Jongen SJ, Vlig M, Nieuwenhuis MK, Middelkoop E et al (2011) Efficacy of skin stretching for

burn scar excision: a multicenter randomized controlled trial. Plast Reconstr Surg 127(5):1958–1966
15. Freeman LJ, Pettit GD, Robinette JD, Lincoln JD, Person MW (1987) Tissue reaction to suture material in the feline linea alba: a retrospective, prospective, and histologic study. Vet Surg. 16(6):440–445
16. Tapan M, Igde M, Yildirim AR, Yasar B, Ergani HM, Duru C (2018) Reverse thenar perforator flap for large palmar and digital defects. J Hand Surg Am 43(10):956e1–956e6
17. Ji X, Liu GM, Cui YT, Jia WY, Luo YG, Cheng ZQ (2020) A hybrid system of hydrogel/frog egg-like microspheres accelerates wound healing via sustained delivery ofRCSPs. J Appl Polym Sci 137(46):49521
18. Zhao Y, Li Z, Song S, Yang K, Liu H, Yang Z et al (2019) Skin-inspired antibacterial conductive hydrogels for epidermal sensors and diabetic foot wound dressings. Adv Funct Mater 29(31):1901474
19. Lear W, Blattner CM, Mustoe TA, Kruzic JJ (2019) In vivo stress relaxation of human scalp. J Mech Behav Biomed Mater 97:85–89
20. Hussain SH, Limthongkul B, Humphreys TR (2013) The biomechanical properties of the skin. Dermatol Surg 39(2):193–203
21. Pamplona DC, Weber HI, Leta FR (2014) Optimization of the use of skin expanders. Skin Res Technol 20(4):463–472
22. Wood JMB, Soldin M, Shaw TJ, Szarko M (2014) The biomechanical and histological sequelae of common skin banking methods. J Biomech 47(5):1215–1219
23. Beltran-Frutos E, Ferrer C, Seco-Rovira V, Martinez-Hernandez J, Serrano-Sanchez MI, Pastor LM (2021) Differences in the response in the dermis of the tails of young and old SD rats to treatment with bipolar RF. J Cosmet Dermatol 20(8):2519–2526
24. Yamawaki Y, Mizutani T, Okano Y, Masaki H (2021) Xanthophyll carotenoids reduce the dysfunction of dermal fibroblasts to reconstruct the dermal matrix damaged by carbonylated proteins. J Oleo Sci 70(5):647–655
25. Elsner P (2003) What textile engineers should know about the human skin. Curr Probl Dermatol 31:24–34
26. Derler S, Gerhardt LC (2012) Tribology of skin: review and analysis of experimental results for the friction coefficient of human skin. Tribol Lett 45(1):1–27
27. Annaidh AN, Bruyere K, Destrade M, Gilchrist MD, Maurini C, Ottenio M et al (2012) Automated estimation of collagen fibre dispersion in the dermis and its contribution to the anisotropic behaviour of skin. Ann Biomed Eng 40(8):1666–1678
28. Pawlaczyk M, Lelonkiewicz M, Wieczorowski M (2013) Age-dependent biomechanical properties of the skin. Postepy Dermatol Alergol 30(5):302–306
29. Topaz M, Ashkenazi I, Barzel O, Biswas S, Atar D, Shadmi N et al (2021) Minimizing treatment complexity of combat-related soft tissue injuries using a dedicated tension relief system and negative pressure therapy augmented by high-dose in situ antibiotic therapy and oxygen delivery: a retrospective study. Burns Trauma. https://doi.org/10.1093/burnst/tkab007
30. Bai HT, Kyu-Cheol N, Wang ZH, Cui YT, Liu H, Liu H et al (2020) Regulation of inflammatory microenvironment using a self-healing hydrogel loaded with BM-MSCs for advanced wound healing in rat diabetic foot ulcers. J Tissue Eng. https://doi.org/10.1177/2041731420947242